



Research
New Technology of Tumor Diagnosis and Treatment—Article

A Smart Procedure for the Femtosecond Laser-Based Fabrication of a Polymeric Lab-on-a-Chip for Capturing Tumor Cell



Annalisa Volpe^{a,b,*}, Udith Krishnan^a, Maria Serena Chiriaco^{c,*}, Elisabetta Primiceri^c, Antonio Ancona^b, Francesco Ferrara^{c,d}

^a Department of Physics, University of Bari “Aldo Moro”, Bari 70126, Italy

^b Institute for Photonics and Nanotechnologies, Bari 70126, Italy

^c Institute of Nanotechnology, Lecce 73100, Italy

^d STMicroelectronics, Lecce 73100, Italy

ARTICLE INFO

Article history:

Received 25 June 2020

Revised 13 October 2020

Accepted 29 October 2020

Available online 1 December 2020

Keywords:

Lab-on-a-chip

Fs laser

Circulating tumor cells

Point of care

Thermal bonding

Polymers

ABSTRACT

Rapid prototyping methods for the design and fabrication of polymeric labs-on-a-chip are on the rise, as they allow high degrees of precision and flexibility. For example, a microfluidic platform may require an optimization phase in which it could be necessary to continuously modify the architecture and geometry; however, this is only possible if easy, controllable fabrication methods and low-cost materials are available. In this paper, we describe the realization process of a microfluidic tool, from the computer-aided design (CAD) to the proof-of-concept application as a capture device for circulating tumor cells (CTCs). The entire platform was realized in polymethyl methacrylate (PMMA), combining femtosecond (fs) laser and micromilling fabrication technologies. The multilayer device was assembled through a facile and low-cost solvent-assisted method. A serpentine microchannel was then directly biofunctionalized by immobilizing capture probes able to distinguish cancer from non-cancer cells without labeling. The low material costs, customizable methods, and biological application of the realized platform make it a suitable model for industrial exploitation and applications at the point of care.

© 2020 THE AUTHORS. Published by Elsevier LTD on behalf of Chinese Academy of Engineering and Higher Education Press Limited Company. This is an open access article under the CC BY-NC-ND license (<http://creativecommons.org/licenses/by-nc-nd/4.0/>).

1. Introduction

Labs-on-a-chip (LoCs), defined as devices in which multiple laboratory techniques are integrated within a chip of a few square centimeters, have tremendous potential for application in various fields of chemistry [1–3] and life sciences, such as in rare cell capturing [4,5]. Among such applications, the capture of circulating tumor cells (CTCs) is one of the most challenging tasks in the field of medical biology [6,7]. The detection of tumor-derived epithelial cells is considered to be one of the most affordable methods to establish the metastatic potential of a tumor, and the presence and number of such cells in blood specimens is a diagnostic and prognostic marker [8]. The possibility of moving LoC technologies into point-of-care (POC) devices for CTC detection is a topic of interest in bedside cancer diagnostics and precision medicine [9]. This technology is recently emerging as a valuable tool for reaching

the ever-increasing number of patients for large-scale screening. In this direction, a number of tests have already been integrated into everyday life through user-friendly tools such as smartphones [10]. Such tests range from blood tests for cardiovascular diseases [11,12] to on-chip nuclear magnetic resonance (NMR) and surface-enhanced raman spectroscopy (SERS) analysis [13,14], and on-chip cell identification [15] through specific dedicated software that can provide counting, detection, and morphometry parameters [16].

Considering the widespread use a POC device could have, polymeric LoCs have generated a huge amount of interest in recent years due to their competitiveness in terms of production costs, production times, and practicality for transitioning an idea into a physical chip [17,18]. Different techniques are achievable for polymeric LoC rapid prototyping [19]. Among these, soft lithography is one of the most exploited methods for prototyping polymeric micro/nanopatterns for microfluidic applications, thanks to its high resolution (<50 nm) [20]. This technology requires the fabrication of a mold, typically by photolithography, whose geometry depends on the target application, replication, and assembling of the entire

* Corresponding authors.

E-mail addresses: annalisa.volpe@uniba.it (A. Volpe), mariaserena.chiriaco@nanotec.cnr.it (M.S. Chiriaco).

device. A significant limitation of this technique is the material used; polydimethylsiloxane (PDMS) suffers from deformation when subjected to high liquid pressures in microchannels [21]. Moreover, like all photolithography-based techniques, soft lithography is a time-consuming process, which often limits optimization in prototyping or iterative design. During the design of a new device, technologies that are based on the direct microstructuring of the substrate—that is, techniques that do not require molds—are much more convenient. Among such technologies are direct laser writing (DLW) methods and three-dimensional (3D) printing to name just a few. The latter has obvious attractions, given its potential to be exploited in the field of LoCs and the possibility of fabricating truly 3D microfluidic devices in a single step from a computer model, given the low price of desktop printers. Despite these benefits, 3D printed structures cannot currently compete with the resolution of structures produced by other direct structuration techniques. Indeed, its applicability is limited by the technical inability to reliably print microfluidic channels with dimensions less than several hundred microns in a reasonably sized device. There are also concerns regarding dimensional fidelity, shape conformity, surface quality, optical transparency, and material availability [22]. Conversely, the flexibility of ultrafast laser technology enables the rapid prototyping and high-precision micromachining of LoC devices with complex microfluidic channel networks [23,24], without a need for the expensive masks and facilities required by the lithographic process. Furthermore, the ability of femtosecond (fs)-laser pulses to produce “cold” ablation of the irradiated volume, thereby avoiding debris and recast layers without restriction of the substrate materials, makes this technology particularly suitable for microfluidic device fabrication [25–28], even though its cost is higher than those of other traditional techniques. In comparison with DLW, mechanical micromilling is more convenient for large features [29] and is a flexible, cost-efficient, and rapid prototyping technology for polymer devices; however, it results in poor surface quality and is unsuitable for optical detection in microchannels [30].

Regardless of how a microfluidic pattern has been fabricated, a further step involves the bonding of the structured substrates or layers with a cover plate in order to obtain effectively sealed microchannels. In the literature, complex equipment has been presented for the controlled evaporation of solvents in order to obtain a surface modification that aids the thermal-assisted sealing of polymers [31]. Other research groups have made use of thermal annealing, adhesive coating, or plasma activation of surfaces and subsequent pressure bonding [32–34]. For example, a solvent-assisted method for bonding polymethyl methacrylate (PMMA)–PMMA devices has been published, which was based on the exposure of substrates to acetone vapors. However, the authors reported that modification of the roughness due to this solvent affected the application of the device as a microfluidic tool [33].

Volpe et al. [35] demonstrated the feasibility of bonding polymeric LoCs through fs-laser welding. In their study, a laser beam that was focalized at the interface of two transparent substrates generated nonlinear absorption and, consequently, local melting and resolidification of the material. Although these methods are effective, they are not suitable for low-cost and quick fabrication requiring expensive equipment and/or complex alignment procedures. On the other hand, although thermal bonding methods represent a very low-cost alternative, they are based on polymer melting and are not suitable for bonding patterned substrates with very small channel sizes, as deformation or blocking of the channels is highly probable during the heating process. Thus, low-temperature (under 90 °C) processes are preferable [36].

In this work, we develop and test a new smart procedure for the rapid prototyping of a PMMA LoC for cell capture by exploiting

fs-laser technology for the microchannel mechanical micromilling for inlet and outlet connections, and thermal bonding to complete the device. Among the many different polymers used in microfluidics, PMMA is the most commonly used, due to its favorable optical, mechanical, and chemical characteristics, which include transparency, good thermal stability, chemical inertness, and high hydrophobicity, as well as its mechanical stability in laser ablation and micromilling processes [37].

Starting from a computer-aided design (CAD) file, the combination of fs-laser ablation and micromilling manufacturing technologies offers ample adaptability to rapidly create and test different fluidic designs and optimize the cell capturing strategy, taking advantage of the micrometric precision and high flexibility of ultrashort-pulse micromachining while maintaining a sustainable development cost.

An easy and cost-effective thermal- and solvent-assisted bonding method for assembling polymeric chips is also included in the protocol [38], which demonstrates some of the innovative features of this low-cost and easy procedure. The procedure, which was established for PMMA–PMMA and is based on the use of common solvents, low temperatures, and low pressures, makes it possible to obtain strong adhesion and robust devices while retaining the desired shape and transparency of the fabricated microchannels.

As a proof of application, the device has been demonstrated to be useful for the label-free capturing and identification of tumor cells from blood cells. Toward this aim, after the fabrication of a serpentine microchannel, we performed an “in-flow” biological functionalization of the inner walls of the channel using anti-epithelial cell adhesion molecule (EpcAM) antibodies, which are able to distinguish cancer from non-cancer cells by recognizing the antigen of the epithelial membrane of oral carcinoma cells and blocking them on the channel walls. In principle, the complete transparency of the entire device permits the identification of cells that have been immobilized within the channels, with no need for further labeling with fluorescent antibodies. Indeed, the characterization of captured cells depends on the immobilized antibody on the channel walls. In our case, we demonstrated that only tumor cells are recognized by an antibody directed toward a membrane antigen that is typical of cancer, and the tumor cells can be clearly glimpsed in the channels. The serpentine shape of the channel allows the sample to pass along a prolonged path, which helps to maximize the interactions between the cells and antibodies. The total volume of sample contained in the channel at a given moment is very low (a few microliters), but considering the in-flow operation, this configuration would be useful for the on-chip collection of rare cells and the enrichment of a sample starting from a higher volume (i.e., milliliters).

2. Materials and methods

2.1. Materials

The device was fabricated on PMMA substrates (Vistacryl CQ; Vista Optics, Ltd., UK) with optical surface quality (measured surface roughness (R_a) < 5 nm). The plates were square, with a length and width of 25 mm and a thickness of 5 mm for the upper layer and 1 mm for the bottom one.

For microchannel functionalization, we used 3-aminopropyltriethoxysilane (APTES; 5%) in ethanol, glutaraldehyde (0.05%) in water, bovine serum albumin (BSA) (1%) and Tween®20 (0.05%) in phosphate-buffered saline (PBS), and anti-EpcAM mouse monoclonal antibodies (all reagents from Sigma-Aldrich, USA). The anti-EpcAM antibodies specifically recognize human EpcAM expressed on the surface of epithelial cells and are not reactive with normal or neoplastic non-epithelial cells.

The OECM-1 human oral squamous carcinoma cell line (purchased from SCC/Sigma-Aldrich, USA) is suitable for studies of cancer cell signaling, epithelial-mesenchymal transition (EMT), metastasis, invasion, and cancer cell stemness. Jurkat cell lines (purchased from ATCC, USA) are human blood (leukemic T-cell lymphoblast)-derived cells.

2.2. Fabrication, functionalization, and testing of the LoC

The serpentine channel was designed using Rhinoceros 5 CAD software (Robert McNeel & Associates, USA) and fabricated with a 1030 nm laser ultrafast solid-state laser system (mod. TruMicro Femto Ed.; TRUMPF GmbH+Co. KG, Germany) based on the chirped pulse amplification technique. The laser source provides an almost diffraction-limited beam ($M^2 < 1.3$) linearly polarized with a pulse duration of 900 fs. A quarter-wave plate circularly polarizes the beam, which is then focused and moved onto the polymeric surface through a galvo-scan head (IntelliSCANNse 14; SCAN-LAB, Germany) equipped with a telecentric lens with a focal length of 100 mm, providing a spot diameter at the focusing point of about 25 μm . Although PMMA is almost transparent at the laser wavelength, thanks to the high peak fluence of the focused fs-laser pulses, nonlinear multiphoton absorption mediates the coupling of the laser light with the transparent polymer, allowing the gentle ablation of a thin surface layer along the irradiation path. The layer-by-layer milling procedure was performed by superimposing two perpendicular scanning patterns. The lateral distance between two parallel scanning lines was 5 μm . A repetition rate (RR) of 50 kHz, a pulse energy of 12 μJ , and a scan speed of 40 $\text{mm}\cdot\text{s}^{-1}$ were selected. After the micromachining process, loosely attached debris was removed by ultrasonic cleaning in distilled water for 10 min. The dimensions of the fs-laser milled microfeatures and the average roughness, R_a , of the milled surface were measured by an optical microscope (Eclipse ME600; Nikon, Japan) and an optical ContourGT InMotion (Bruker, USA) profilometer, respectively.

The inlet and outlet were designed using Rhinoceros 5 CAD software, and CAD-computer-aided manufacturing (CAM) software was used to transfer the CAD information in machine code file for the micromilling control. The inlet and outlet were aligned with the serpentine channel using the on-board camera of the micromilling machine (Mini-Mill/GX; Minitech Machinery, USA). A 400 μm tool was used to mill the PMMA layer at 20 000 revolutions per minute (RPM) with air cooling.

To bond the PMMA layers, hot, pure isopropyl alcohol (70 $^{\circ}\text{C}$) was deposited in a protected environment using a spin coater set at 2000 RPM for 10 s on the flat bottom substrate; the excess was eliminated with blotting paper. The two PMMA slices were then assembled. The position was held with binder clips and the device was then immediately transferred to an oven at 60 $^{\circ}\text{C}$, where it remained for 20 min without additional pressure.

The assembled device was connected to perfectly fitting capillary tubes with micromilled shaped inlets and outlets, and connected to the microfluidic setup. The Elveflow micropumping system (Elvesys, France) that was used is equipped with an OB1 base module, two MkIII+ channels for the pressure controller, and two microfluidic flow sensors. A sequence of solutions was injected into the serpentine channels, starting with APTES (5%) in ethanol. This step resulted in the incorporation of amine functionality and the hydrophilization of the PMMA surface. The PMMA was grafted by means of a condensation reaction of the surface with the silanol group of the APTES, which created amine-functionalized PMMA (PMMA-NH₂). This made the PMMA channels hydrophilic, which allowed easier flowing of the subsequent water-based solutions. After washing the channels with water, glutaraldehyde (0.05%) was injected, which interacted with the

amine-activated group to produce PMMA-glutaraldehyde. In the subsequent phase, the latter underwent an imine coupling reaction with the amine group of the antibody, thus achieving immobilization of the anti-EpCAM antibody [39,40]. A passivation step with a blocking buffer (BSA-Tween[®]20 in PBS) was performed to prevent unspecific cell adsorption. For real-time acquisition during the capture test, an Olympus IX81 inverted microscope (Japan) was used. This setup includes an Okolab system equipped with a temperature-controlled box and a camera. Cell cultures were grown in an incubator at 37 $^{\circ}\text{C}$ with 5% CO₂ and were cultured in suspension (Jurkat cells) in RPMI 1640 complete growth medium (Sigma-Aldrich); or in adhesion (OECM-1 cells) in complete Dulbecco's Modified Eagle's Medium (DMEM; Sigma-Aldrich); the medium was renewed every two days. A few minutes before the capture experiments, the cancer cells were suspended and harvested using 0.05% trypsin. After detachment, the cells were washed and resuspended in DMEM medium at the right dilution. The Jurkat cells were collected from the flask, centrifuged, counted, and resuspended at the right dilution. The solutions were then loaded into capillary tubes using the microfluidic setup set at a flow velocity value of 7 $\mu\text{L}\cdot\text{min}^{-1}$.

3. Results

3.1. Fabrication of the LoC device

The first step in the realization of the device was the CAD of its elements, which was then transferred in machine code to the fabrication instruments used. Figs. 1(a) and (b) schematically illustrates the proposed geometry. Various different architectures of the device were designed and tested in order to optimize the parameters of fabrication, bonding, and final application. Here, we discuss the final layout of the device, which is based on a serpentine microchannel with a square cross-section of 100 μm per side and a total length of 180 mm to increase the active path and therefore increase the probability of capturing cells. Two PMMA substrates were used in order to minimize the dimensions of the assembled device and obtain transparency. The upper substrate (Fig. 1(a)) was machined separately on the two faces. On the lower face, the serpentine-shaped channel was fabricated by fs-laser ablation, which gently removed the material layer by layer with micrometric precision until the designed depth was reached. On the upper face, the inlet and outlet drilled holes were made using the micromilling machine. The bottom layer was a flat and smooth PMMA substrate that was just used to seal the channel (Fig. 1(a)).

The inlet and outlet were made using a mechanical micromilling machine mounting a 400 μm tool, after careful alignment with the serpentine ends on the opposite face. The air-cooled milling was accomplished at a feed rate of 100 $\text{mm}\cdot\text{min}^{-1}$ and a spindle speed of 20 000 RPM according to Reichenbach et al. [41]. The inlet and outlet were concentric cylinder holes that fit perfectly with the external and internal dimensions of the capillary. From the center of these cylinders, channels with a diameter of 600 μm and a length of 5 mm were realized, which allowed the fluids injected from the opposite face to reach the serpentine channel.

Fig. 2(a) shows a stereoscopic image of the micromachined serpentine channel. In Fig. 2(b), a particular portion of the device is highlighted. The edge of the channel showed no cracks, burrs, or recast layers that could hinder the sealing procedure. The bottom part of the channel had a roughness, R_a , of about 2 μm . This value was negligible compared with the channel height; therefore, it did not affect the fluidic transport of the cells. The substrates were treated with an ultraviolet (UV) plasma process in order to remove the milling process residuals and create hydrophilicity.

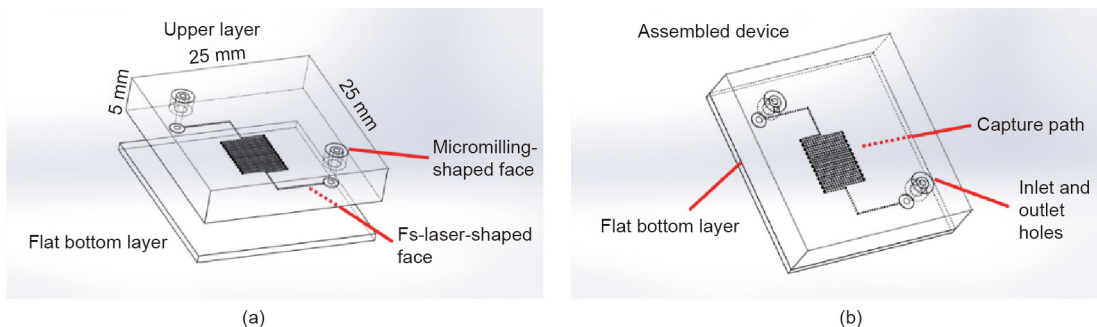


Fig. 1. (a) The modules of the PMMA device: The upper layer has been milled on both sides to obtain an fs-laser-shaped serpentine channel on the bottom and micromilling machine inlet and outlet holes on the top. A flat slice of PMMA seals the serpentine channel. (b) The architecture of the assembled device.

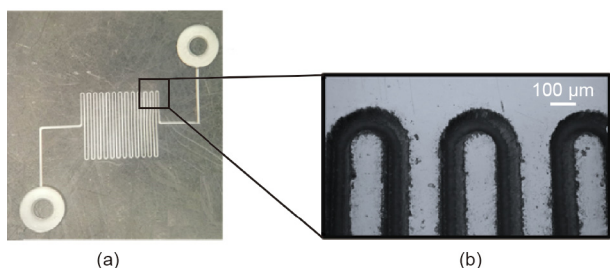


Fig. 2. (a) Stereoscopic image of the laser micromachined sample; (b) microscopic 3D detail of the serpentine channel.

3.2. Bonding and functionalization of the device

A thermal- and solvent-assisted bonding method was developed to assemble the microfluidic device. Hot isopropyl alcohol was deposited in a protected environment on the flat substrate. The two PMMA slices were then placed together; their position was held with clamps, and the device was then immediately transferred to the oven. Once the device was assembled, it was connected to the micropumping system by capillary tubes; as can be seen from Fig. 3(a), no additional glue, luer fittings, or gaskets were necessary for a watertight seal. In this way, a “plug-and-play” operating system was realized, that avoided the typical sealing problems of microfluidic devices. The in-flow functionalization was performed through the serpentine channel, followed by optical microscope monitoring (see the sequence in Fig. 3(b)). The complete transparency of the device permitted reproducibility of the assay and online monitoring of the flow

injection. A specific protocol for PMMA channel functionalization was optimized, including filling with a solution of APTES (5%) in ethanol, followed by the injection of glutaraldehyde (0.05%) in water, and then the injection of a solution of anti-EpCAM antibody in PBS. The serpentine shape of the channel, combined with the slow flow rate of the solutions ($7 \mu\text{L}\cdot\text{min}^{-1}$) and the real-time monitoring of the filling, allowed us to obtain a tool able to exploit a very high surface/volume ratio in terms of active binding sites for antibodies and, consequently, with excellent cell capturing abilities.

3.3. CTC capture experiments

The ability of the microfluidic device to distinguish cancer cells from normal cells was tested. For this reason, in the last step, we immobilized the anti-EpCAM antibody, which is able to recognize human EpCAM, a membrane biomarker that is typically present on the surface of epithelial-type cancer cells [42,43]. A final passivation step to avoid unspecific cell absorption was then performed, which involved rinsing with a PBS buffer containing BSA (1%) and Tween®20 (0.05%), followed by PBS rinsing. In order to demonstrate the effectiveness of our device and propose an application proof for the assembled device, we spiked culture medium samples with two different populations of cells (blood and tumor cells) in order to simulate the content of a complex real sample. In particular, we used Jurkat cells (blood-derived cells) and the OECM-1 human oral squamous carcinoma cell line (epithelial-like cells from human oral cancer). We separately prepared 5 mL suspensions of cells containing 1×10^6 cells·mL⁻¹ from the Jurkat line and 1×10^4 cells·mL⁻¹ from the OECM-1 line. The cell suspensions were allowed to slowly flow through the serpentine microchannel

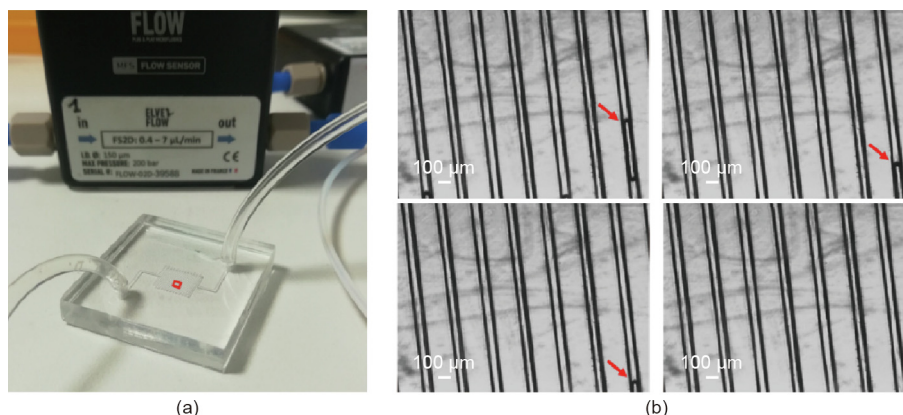


Fig. 3. (a) An image of the final device with a microfluidic connection to the micropump and flow sensors. (b) Monitoring the flow into the microchannels under an optical microscope. The sequence of bubbles generated during injection (indicated by the red arrows) made it possible to follow the serpentine channel functionalization.

with a flow rate of $7 \mu\text{L}\cdot\text{min}^{-1}$. The low velocity of the fluid, the size of the channel, and its serpentine shape were optimized to maximize cell interactions with the internal walls, where antibodies fixed on the surface could recognize cells expressing the membrane epithelial antigen.

In the case of the Jurkat cells, very few or no cells were identified in the channels after washing with PBS solution (Fig. 4). Indeed, the Jurkat cells do not express EpCAM antigen on the surface of the cell membrane; thus, they could not be recognized and fixed by the antibodies immobilized on the channel walls. In order to demonstrate the presence of Jurkat cells in the serpentine channel, we opened an additional micromilled hole in the middle of the serpentine channel, where the Jurkat cells quickly accumulated, dragged by fluidic forces (Fig. 5).

In contrast, in the case of the OECM-1 suspension of cells, a large number of cells were captured on the inner walls; they were also found to adhere to the surface after washing with PBS. As shown in Fig. 6, the cells were clearly visible through the transparent PMMA device, confirming the possibility of using such a tool as a diagnostic instrument to immobilize and discriminate cancer cells from normal blood cells in a label-free manner, with no need for a fluorescence detector or complex instruments.

As shown in the high-magnification images, some wrinkles are evident outside of the channel. This is a typical issue that occurs

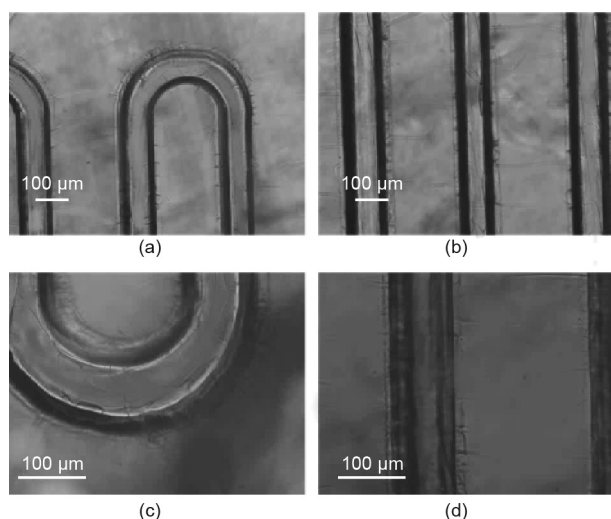


Fig. 4. PMMA microchannels after the flowing of Jurkat cells and subsequent washing in PBS. Few or no cells are visible along the pathway of the microchannel: (a, c) serpentine loop at different magnifications; and (b, d) straight portions of the channel at different magnification.

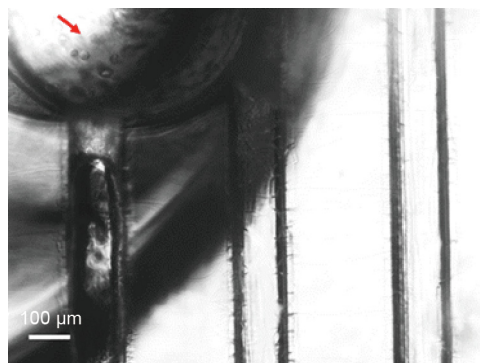


Fig. 5. This image shows the Jurkat cells that accumulated in a hole in the middle of the serpentine channel that was made intentionally in order to verify that this kind of cell does not adhere to the biofunctionalized channel's surface, but rather is dragged by microfluidic forces toward the additional outlet.

with the solvent-assisted bonding of thermoplastic materials; the wrinkles are probably due to the stress induced by the combination of solvent and temperature treatments, as reported in the Ref. [33]. In many reported cases, the presence of cracks is so pronounced that the structure of the channels is affected, which limits the applicability of the device. In our case, however, the wrinkles were present only on the surface of the device, outside of the serpentine microchannel, due to the fact that we only spin-coated the flat PMMA substrate with isopropanol and did not spin-coat the upper layer (Fig. 1(a)). As a result, the isopropanol did not fill in the channels during bonding but only acted on the unmodified portions of the milled plate, which were those that supported adhesion.

4. Discussion

In this work, we realized a microfluidic PMMA device and tested its functionality in capturing tumor cells directly in flow. The device takes advantage of a smart and flexible procedure based on three steps: ① fabrication of the microfluidic network using a hybrid micro-manufacturing platform that combines fs-laser and mechanical micromilling technologies; ② assembly and sealing of the device using a facile and low-cost thermal and solvent-assisted bonding method; and ③ in-flow and on-chip functionalization of the obtained microchannels. The adoption of this procedure makes it possible to easily prototype devices for many different applications. The device presented in this work can be used in a plethora of interesting contexts, as it is a valuable tool not only for the simple study of cells, but also for onsite diagnostics, if embedded in a more complex setup. Indeed, the entire platform has potential to be transferred in the near future into portable systems, through appropriate integration with an optical system to provide high pixel density, faster focusing, and image stabilization [44].

This hybrid micro-fabrication platform benefits from the combination of two advanced manufacturing technologies—ultrafast lasers and mechanical micromilling—that are both extremely flexible and particularly suitable for the rapid prototyping of customizable LoCs. As it is a non-contact technology, fs-laser ablation allows the fabrication of complex geometrical features with negligible collateral damage to the surrounding material; in addition, it provides micrometric precision thanks to the possibility of focusing the laser radiation in a diffraction-limited spot. Furthermore, the use of mechanical micromilling makes it possible to significantly reduce processing times, especially when manufacturing large and/or simple features (e.g., holes) that do not require high levels of precision. One of the principal drawbacks of inlet and outlet in microfluidic chips is that it can often be challenging to perfectly seal tubes without relying on the addition of Luer fittings, glues, or other strategies for avoiding leaky connections, which may affect microscope observation. In our case, we obtained the perfect sealing of tubes by customizing the micromilled hole with the presence of an inner pierce, so that a cylindrical hole drives the capillary tube connection without the need for any additional sealing.

The combination of these two techniques makes it possible to overcome the limitations of other technologies more commonly used for the rapid prototyping of LoCs. In fact, unlike soft lithography, the proposed method is suitable for any kind of material and does not require a mold; thus, it offers greater flexibility in the prototyping phase. In addition, it is possible to obtain much more precise structures with this method than with 3D printing, while maintaining a short fabrication time.

We also described an easy and noteworthy low-cost bonding method that does not require glues or additional gaskets, and that is not a disruptive process with aggressive solvents or temperatures. The choice of PMMA as the material to build the entire device is of strong interest due to its low cost, which makes it particularly suitable for industrial exploitation. In comparison with other

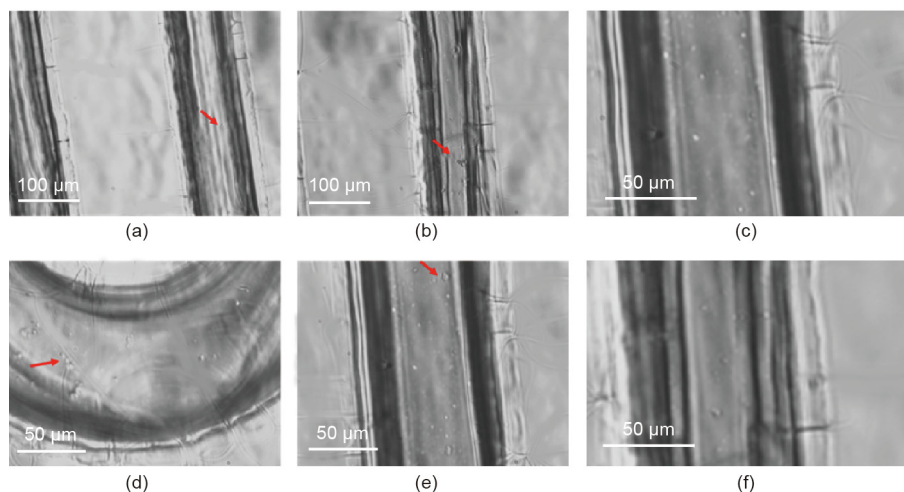


Fig. 6. Microscopic images of the PMMA microchannel with blocked OECM-1 cells after washing with PBS. A large number of cells are captured on the inner surface of the channel, as marked by red arrows in (a) and (b) along the straight portions of the channel. In (c), a higher magnification of (b) is reported. (d) Cells in the serpentine loop; (c, e, and f) zoomed-in regions of channel reported in (b).

polymers that have been used for the manufacture of microfluidic devices (e.g., PDMS), PMMA is stiffer, which ensures better mechanical stability, reproducibility, and durability of the microfluidic network. A non-negligible aspect is the biocompatibility of PMMA, which permits the realization of tools for biological applications ranging from LoCs [45] to prosthesis fabrication [46].

Moreover, the complete transparency of this device has been preserved throughout the fabrication, allowing perfect alignment during multistep procedures and the real-time monitoring of experiments. This feature is of crucial importance for checking the correct filling of channels and following all the steps of an experiment under a microscope lens.

As a proof of concept, we used the assembled device as a tool for CTC detection. The CTC number in blood is highly variable, depending on the stage and aggressivity of a tumor; nevertheless, their detection at an early stage is considered to be a key factor in clinicians' decision-making. This kind of analysis falls within liquid biopsy, which aims to develop increasingly less invasive methods of analysis and to increase patients' compliance. In order to create a tool for CTC detection, we realized a microfluidic channel through rapid prototyping methods and functionalized it with anti-EpCAM antibodies that can bind a membrane protein that is highly expressed on the surface of most epithelial malignant tissues [47]. The recognized EpCAM antigen has a regulatory function in cell-cell adhesion strength and tissue plasticity and plays an important role in epithelial cell proliferation and differentiation. It is considered to be a useful tool in the research of epithelial cells, cancer diagnostics, and the prediction of disease progression [43]. Being able to identify CTCs in a label-free way would be a great achievement in the field of liquid biopsy, as the isolation/counting of cells currently requires complex analysis deriving from cytometry, based on bulky and expensive instruments and on a variety of steps for sample enrichment and labeling [48]. In the present study, we use a microfluidic approach to both functionalize and capture human oral squamous carcinoma cells from a spiked suspension of OECM-1 cell culture medium and realize a positive selection approach thanks to the presence of the immobilized antibody. As expected, blood-derived Jurkat cells flowed through the serpentine channel without being recognized by the capture antibodies, which can only bind cancer cells. The starting volume of our samples was 5 mL, which demonstrated that our device, which holds a total volume of 2 μ L, can be used for the enrichment and concentration of diluted solutions. This finding has a high impact in the field of liquid biopsy, in which CTC are expected to exist in

a very low number, as being able to collect such cells within a small volume or space makes it possible to obtain consistent biological material for further analysis. Moreover, in principle, the architecture of the microfluidic device could be customized to allow, for example, differentiated functionalization for a greater number of channels in order to identify the expression of several membrane biomarkers; the results could then be organized in order to match the greater amount of information coming from the different channels.

5. Conclusions

The paper describes the rapid prototyping of a smart and customizable plastic LoC for capturing CTCs. The device innovatively combines high-precision fs-laser ablation, ease-of-use mechanical micromilling, and a cost-saving solvent-assisted sealing method for PMMA substrates, thereby ensuring the reliability of microfluidic assays. Moreover, the tool facilitates an external microfluidic connection thanks to a specific design of the inlet and outlet holes that permits a capillary watertight connection in a user-friendly plug-and-play device. The optimized process resulted in a completely transparent tool suitable for direct optical investigation and for the dedicated biofunctionalization of the serpentine channel, with the aim of selectively capturing and enriching tumor cells from a biological sample in a completely label-free way. Mobile phones, tablets, or low-cost complementary metal-oxide semiconductor (CMOS) devices can be further integrated for the easy detection of CTCs, leading to a step forward in the field of personalized medicine and on-field diagnostics.

Acknowledgments

This work was supported by SMILE (a SAW-MIP Integrated device for oral cancer Early detection) project, part of the ATTRACT program that has received funding from the European Union's Horizon 2020 Research and Innovation Program (777222).

Authors' contribution

Plan and design of the work: AV, MSC, EP, AA, and FF; experimental activity: AV, UK, MSC, and FF; responsible for experimental setups: AA and FF; implementation of the research, main conceptual ideas, and proof outline: MSC and FF; analysis of results:

MSC, EP, and FF; writing of the manuscript: AV, MSC, and FF; manuscript revisions: AV, UK, MSC, EP, AA, and FF; project supervisors and funding responsibilities: MSC and FF.

Compliance with ethics guidelines

Annalisa Volpe, Udith Krishnan, Maria Serena Chiriaco, Elisabetta Primiceri, Antonio Ancona, and Francesco Ferrara declare that they have no conflict of interest or financial conflicts to disclose.

References

- [1] Cao L, Cui X, Hu J, Li Z, Choi JR, Yang Q, et al. Advances in digital polymerase chain reaction (dPCR) and its emerging biomedical applications. *Biosens Bioelectron* 2017;90:459–74.
- [2] Cereda M, Cocci A, Cucchi D, Raia L, Pirola D, Bruno L, et al. Q3: a compact device for quick, high precision qPCR. *Sensors* 2018;18(8):2583.
- [3] Ocaña-González JA, Fernández-Torres R, Bello-López MÁ, Ramos-Payán M. New developments in microextraction techniques in bioanalysis. A review. *Anal Chim Acta* 2016;905:8–23.
- [4] Qasimeh MA, Wu YCC, Bose S, Menachery A, Talluri S, Gonzalez G, et al. Isolation of circulating plasma cells in multiple myeloma using CD138 antibody-based capture in a microfluidic device. *Sci Rep* 2017;7(1):45681.
- [5] Edd JF, Mishra A, Dubash TD, Herrera S, Mohammad R, Williams EK, et al. Microfluidic concentration and separation of circulating tumor cell clusters from large blood volumes. *Lab Chip* 2020;20(3):558–67.
- [6] Yap TA, Lorente D, Omlin A, Olmos D, de Bono JS. Circulating tumor cells: a multifunctional biomarker. *Clin Cancer Res* 2014;20(10):2553–68.
- [7] Park MH, Reátegui E, Li W, Tessier SN, Wong KHK, Jensen AE, et al. Enhanced isolation and release of circulating tumor cells using nanoparticle binding and ligand exchange in a microfluidic chip. *J Am Chem Soc* 2017;139(7):2741–9.
- [8] Nagrath S, Sequist LV, Maheswaran S, Bell DW, Irimia D, Utkus L, et al. Isolation of rare circulating tumour cells in cancer patients by microchip technology. *Nature* 2007;450(7173):1235–9.
- [9] Primiceri E, Chiriaco MS, Notarangelo FM, Crocamo A, Ardissino D, Cereda M, et al. Key enabling technologies for point-of-care diagnostics. *Sensors* 2018;18(11):3607.
- [10] Guo J. Smartphone-powered electrochemical biosensing dongle for emerging medical IoTs application. *IEEE Trans Industr Inf* 2018;14(6):2592–7.
- [11] Guo J. Uric acid monitoring with a smartphone as the electrochemical analyzer. *Anal Chem* 2016;88(24):11986–9.
- [12] Guo J, Ma X. Simultaneous monitoring of glucose and uric acid on a single test strip with dual channels. *Biosens Bioelectron* 2017;94:415–9.
- [13] Guo J, Jiang D, Feng S, Ren C, Guo J. μ -NMR at the point of care testing. *Electrophoresis* 2020;41(5–6):319–27.
- [14] Guo J, Zeng F, Guo J, Ma X. Preparation and application of microfluidic SERS substrate: challenges and future perspectives. *J Mater Sci Technol* 2020;37:96–103.
- [15] Zhao W, Tian S, Huang L, Liu K, Dong L, Guo J. A smartphone-based biomedical sensory system. *Analyst* 2020;145(8):2873–91.
- [16] Falk T, Mai D, Bensch R, Çiçek Ö, Abdulkadir A, Marrakchi Y, et al. U-Net: deep learning for cell counting, detection, and morphometry. *Nat Methods* 2019;16(1):67–70.
- [17] Pugliese M, Ferrara F, Bramanti AP, Gigli G, Maiorano V. In-plane cost-effective magnetically actuated valve for microfluidic applications. *Smart Mater Struct* 2017;26(4):26.
- [18] Chiriaco MS, Bianco M, Amato F, Primiceri E, Ferrara F, Arima V, et al. Fabrication of interconnected multilevel channels in a monolithic SU-8 structure using a LOR sacrificial layer. *Microelectron Eng* 2016;164:30–5.
- [19] Abgrall P, Gué AM. Lab-on-chip technologies: making a microfluidic network and coupling it into a complete microsystem—a review. *J Micromech Microeng* 2007;17(5):R15–49.
- [20] Schönleber A, van Smaalen S, Larsen FK. Orientational disorder in Λ -cobalt (III) sepulchrate trinitrate. *Acta Crystallogr C* 2010;66(Pt 4):m107–9.
- [21] Gervais T, El-Ali J, Günther A, Jensen KF. Flow-induced deformation of shallow microfluidic channels. *Lab Chip* 2006;6(4):500–7.
- [22] Waheed S, Cabot JM, Macdonald NP, Lewis T, Guijt RM, Paull B, et al. 3D printed microfluidic devices: enablers and barriers. *Lab Chip* 2016;16(11):1993–2013.
- [23] Volpe A, Paiè P, Ancona A, Osellame R. Polymeric fully inertial lab-on-a-chip with enhanced-throughput sorting capabilities. *Microfluid Nanofluid* 2019;23(3):37.
- [24] Volpe A, Gaudioso C, Ancona A. Sorting of particles using inertial focusing and laminar vortex technology: a review. *Micromachines* 2019;10(9):594.
- [25] Sima FN, Sugioka K, Vazquez RM, Osellame R, Kelemen L, Ormos P. Three-dimensional femtosecond laser processing for lab-on-a-chip applications. *Nanophotonics* 2018;7(3):613–34.
- [26] Wang H, Zhang YL, Wang W, Ding H, Sun HB. On-chip laser processing for the development of multifunctional microfluidic chips. *Laser Photonics Rev* 2017;11(2):1600116.
- [27] Martínez Vázquez R, Trotta G, Volpe A, Bernava G, Basile V, Paturzo M, et al. Rapid prototyping of plastic lab-on-a-chip by femtosecond laser micromachining and removable insert microinjection molding. *Micromachines* 2017;8(11):328.
- [28] Trotta G, Volpe A, Ancona A, Fassi I. Flexible micro manufacturing platform for the fabrication of PMMA microfluidic devices. *Journal of Manuf Process* 2018;35:107–17.
- [29] Faustino V, Catarino SO, Lima R, Minas G. Biomedical microfluidic devices by using low-cost fabrication techniques: a review. *J Biomech* 2016;49(11):2280–92.
- [30] Guckenberger DJ, de Groot TE, Wan AMD, Beebe DJ, Young EWK. Micromilling: a method for ultra-rapid prototyping of plastic microfluidic devices. *Lab Chip* 2015;15(11):2364–78.
- [31] Ogończyk D, Wagrzyn J, Jankowski P, Dabrowski B, Garstecki P. Bonding of microfluidic devices fabricated in polycarbonate. *Lab Chip* 2010;10(10):1324–7.
- [32] Klank H, Kutter JP, Geschke O. CO₂-laser micromachining and back-end processing for rapid production of PMMA-based microfluidic systems. *Lab Chip* 2002;2(4):242–6.
- [33] Matellan C, del Rio HA. Cost-effective rapid prototyping and assembly of poly(methyl methacrylate) microfluidic devices. *Sci Rep* 2018;8(1):8.
- [34] Yu H, Chong ZZ, Tor SB, Liu E, Loh NH. Low temperature and deformation-free bonding of PMMA microfluidic devices with stable hydrophilicity via oxygen plasma treatment and PVA coating. *RSC Adv* 2015;5(11):8377–88.
- [35] Volpe A, Di Niso F, Gaudioso C, De Rosa A, Vázquez RM, Ancona A, et al. Welding of PMMA by a femtosecond fiber laser. *Opt Express* 2015;23(4):4114–24.
- [36] Vlachopoulou ME, Tserepi A, Pavli P, Argitis P, Sanopoulou M, Misiakos K. A low temperature surface modification assisted method for bonding plastic substrates. *J Micromech Microeng* 2009;19(1):19.
- [37] Ali U, Karim KJBA, Buang NA. A review of the properties and applications of poly(methyl methacrylate) (PMMA). *Polym Rev* 2015;55(4):678–705.
- [38] Bamshad A, Nikfarjam A, Khaleghi H. A new simple and fast thermally-solvent assisted method to bond PMMA–PMMA in micro-fluidics devices. *J Micromech Microeng* 2016;26(6):065017.
- [39] Pipatpanukul C, Amarit R, Somboonkaew A, Sutapun B, Vongsakulyanon A, Kitpoka P, et al. Microfluidic PMMA-based microarray sensor chip with imaging analysis for ABO and RhD blood group typing. *Vox Sang* 2016;110(1):60–9.
- [40] Fixe F, Dufva M, Telleman P, Christensen CBV. Functionalization of poly(methyl methacrylate) (PMMA) as a substrate for DNA microarrays. *Nucleic Acids Res* 2004;32(1):e9.
- [41] Reichenbach IG, Bohley M, Sousa FJP, Aurich JC. Micromachining of PMMA—manufacturing of burr-free structures with single-edge ultra-small micro end mills. *Int J Adv Manuf Technol* 2018;96(9–12):3665–77.
- [42] Boral D, Vishnoi M, Liu HN, Yin W, Sprouse ML, Scamardo A, et al. Molecular characterization of breast cancer CTCs associated with brain metastasis. *Nat Commun* 2017;8(1):196.
- [43] Winter MJ, Nagtegaal ID, van Krieken JHJM, Litvinov SV. The epithelial cell adhesion molecule (Ep-CAM) as a morphoregulatory molecule is a tool in surgical pathology. *Am J Pathol* 2003;163(6):2139–48.
- [44] Wei Q, Luo W, Chiang S, Kappel T, Mejia C, Tseng D, et al. Imaging and sizing of single DNA molecules on a mobile phone. *ACS Nano* 2014;8(12):12725–33.
- [45] Kuan DH, Wang IS, Lin JR, Yang CH, Huang CH, Lin YH, et al. A microfluidic device integrating dual CMOS polysilicon nanowire sensors for on-chip whole blood processing and simultaneous detection of multiple analytes. *Lab Chip* 2016;16(16):3105–13.
- [46] Srinivasan M, Gjengedal H, Cattani-Lorente M, Moussa M, Durual S, Schimmel M, et al. CAD/CAM milled complete removable dental prostheses: an *in vitro* evaluation of biocompatibility, mechanical properties, and surface roughness. *Dent Mater J* 2018;37(4):526–33.
- [47] Markou A, Lazaridou M, Paraskevopoulos P, Chen S, Świerczewska M, Budna J, et al. Multiplex gene expression profiling of *in vivo* isolated circulating tumor cells in high-risk prostate cancer patients. *Clin Chem* 2018;64(2):297–306.
- [48] Lowes LE, Goodale D, Keeney M, Allan AL. Image cytometry analysis of circulating tumor cells. In: Darzynkiewicz Z, Holden E, Orfao A, Telford W, Wlodkovic D, editors. *Methods in cell biology*. New York: Academic Press; 2011. p. 261–90.